Journal of
Ceramic Science
and Technology

J. Ceram. Sci. Technol., **09** [3] 337-344 (2018)
DOI: 10.4416/JCST2018-00023
available online at: http://www.ceramic-science.com

Impact of Ba^{2+}on Structure and Electrical Properties of 0.65PMN-0.35PT Ceramics

C. Lu[1, 2], Y. Liu*[1, 2], C. Lyu[1, 2], F. Chen[1, 2], H. Xi[1, 2], Y. Lyu*[1, 2, 3]

[1]The State Key Laboratory of Materials-Oriented Chemical Engineering, College of Materials Science and Engineering, Nanjing Tech University, Nanjing 210009, China
[2]Jiangsu Collaborative Innovation Center for Advanced Inorganic Function Composites, China.
[3]Jiangsu National Synergetic Innovation Center for Advanced Materials (SICAM), China

received March 13, 2018; received in revised form April 24, 2018; accepted May 29, 2018

Abstract

Ba-doped PMN-0.35PT (PMN-0.35PT-*x*Ba) (x = 0 – 0.05) relaxor ferroelectric ceramics were prepared with a two-step columbite precursor method. The effect of using Ba^{2+} to modify the structure and electrical properties of PMN-0.35PT-*x*Ba ceramics near the morphotropic phase boundary was investigated. The introduction of Ba dopant significantly improved the densification of the ceramics and the growth of the grain, but also profoundly modified the phase structure. The study demonstrated that the substitution of Ba main doping for A-site in the PMN-0.35PT lattice could affect electrical properties of PMN-0.35PT binary ceramics. Increasing the dosage of Ba led to enhancement of the ferroelectric response and remarkably increased the electrostrictive response. Results in this study indicated that at a composition *x* of 3.0 mol%, a large strain response could be obtained with maximum strain as high as 0.13 % under the low field of 15 kV/cm at room temperature. The maximum piezoelectric performance is found at x = 0.05 (d_{33} = 508pC/N).

Keywords: PMN-PT, strain, piezoelectric properties, morphotropic phase boundary, phase transition

I. Introduction

Relaxor materials have been extensively studied for almost 60 years since the complex perovskite structure $Pb(Mg_{1/3}Nb_{2/3})O_3$ (PMN) relaxor was first discovered and proposed by Smolenskii [1]. The compounds with chemical composition of (1-x)[$Pb(Mg_{1/3}Nb_{2/3})O_3$]-x[$PbTiO_3$] (PMN-PT) are pseudo-binary relaxor ferroelectric materials with excellent piezoelectric, dielectric, and ferroelectric properties, which makes the compounds attractive for applications like electromechanical actuators and sensors[2, 3]. As we know, PMN-PT ferroelectrics have a perovskite-type structure with a morphotropic phase boundary (MPB) around a composition of $x = 0.35$ at room temperature[4–6], and in the vicinity of the MPB, piezoelectric ceramics show good piezoelectricity. The ceramics of PMN-PT have been reported to possess an extra-high electromechanical coupling factor and piezoelectric coefficient with the MPB, making it a very promising candidate for piezoelectric actuator and transducer applications.

Recently, ternary $Pb(In_{1/2}Nb_{1/2})O_3$-(1-x-y)$Pb(Mg_{1/3}Nb_{2/3})O_3$-x$PbTiO_3$ (PIN-PMN-PT) ceramics near MPB have shown comparable electromechanical properties (d_{33}~500pC/N) [7–10] and higher strain with 0.1 % in a low field of 15 kV/cm at room temperature[11]. However, concerns about the stability of piezoelectric ceramics prevent the industrial development of relaxor ferroelectrics based on multicomponent ceramics[12–14]. The instability of the perovskite structure is mainly due to the formation of non-ferroelectric in the focal process in the synthesis of the stone material phase (e.g. $PbNb_2O_7$ [15]), in which the piezoelectric and dielectric properties decrease significantly. The partial substitution of barium in the lattice of the perovskite structure is a method of maintaining the stability of the perovskite structure. With smaller electronegativity and polarizing effect as well as a large ionic radius compared to Pb^{2+}, Ba^{2+}cations lead to a lower degree of covalence of the A-O bonds [16, 17].

In this work, Ba-doped PMN-0.35PT (PMN-0.35PT-*x*Ba)(x=0 – 0.05) relaxor ferroelectric ceramics were prepared with the two-step columbite precursor method. On one hand, the stability of 0.65PMN-0.35PT ceramic phase structure can be enhanced by barium ion doping. On the other hand, Ba-doped 0.65PMN-0.35PT ceramics can improve their strain and piezoelectric properties under the low field of 15 kV/cm.

II. Experimental Procedure

Ba-doped 0.65$Pb(Mg_{1/3}Nb_{2/3})O_3$-0.35$PbTiO_3$ (PMN-0.35PT-*x*Ba, *x* = 0.0, 2.0, 3.0, 4.0, and 5.0 mol%) ceramics were prepared by means of conventional solid-state sintering with a two-step precursor method. The niobium magnesium niobate precursor ($MgNb_2O_6$) was synthesized based on the calcination of MgO (98.5 %) and Nb_2O_5

* Corresponding author: yfliu@njtech.edu.cn
co-corresponding author: yinonglu@njtech.edu.cn

(99.5 %) at 1 000 °C for 4 h with an excess of 1 mol% of MgO in order to suppress the pyrochlore phase. Then stoichiometric amounts of PbO (99.0 %), TiO_2 (99.5 %), $BaCO_3$(98.0 %) were doped and mixed into the above precursor $MgNb_2O_6$. The mixture was batched and wet-milled for 12 h in ethanol in a planetary ball mill. At the same time, an excess of 1 wt% PbO was added to compensate for PbO volatility during calcination and sintering. Then the dried mixtures were calcined at 850 °C for 2 h and wet-milled for 16 h in the same process as described previously. The dried powders were mixed with 5 wt% polyvinyl alcohol (PVA) binder and dry-pressed into pellets. After the binder had been burned out at 600 °C, the green compacts were sintered at 1 200 °C for 2 h in a sealed alumina crucible. To compensate for PbO evaporation during sintering, a PbO-rich atmosphere was maintained by placing counterpart PMN-0.35PT powders in the crucible.

The phase of the sintered ceramics was characterized with the X-ray diffraction technique (Smartlab 3 kW, Rigaku, Japan) with CuKα radiation. The fracture surface micromorphology of the ceramics was imaged with a scanning electron microscope (SEM, JSM-6510, JEOL, Japan) with the energy-dispersive X-ray technique (EDS, Thermo, American). The average grain size of the ceramics was determined with a linear interception method on SEM micrographs. The bulk density of all the ceramic specimens was evaluated with the Archimedes method. Before the electrical properties were studied, the specimens were polished parallel and coated on both sides with silver paint as electrode, and then fired at 750 °C for 0.5 h. In a Radiant Technology Precision Premium II tester (Precision Premier II, American) connected to an accessory laser interferometer vibrometer, the P-E hysteresis loops and S-E strain curves were plotted under a field of 15 kV/cm with a frequency of 0.1 Hz at room temperature. The piezoelectric charge coefficient d_{33} was measured using a piezo-d_{33}meter (ZJ-3A, Institute of Acoustics of China Academy of Sciences) after poling at 120 °C for 30 min at an applied electric field of 4 kV/mm.

III. Results and Discussion

(1) Phase structure and microstructure

Fig. 1a shows the XRD patterns of PMN-0.35PT ceramics with different Ba-doped content. The peak positions and intensities of XRD patterns were changed with the amount and chemical composition of the phases present. From the XRD patterns, the PMN-PT ceramic was identified as a single-phase material with a perovskite structure having tetragonal symmetry. As shown in Fig. 1(b), with increasing Ba ion content, the diffraction peak around a 2θ value of 44°-46° shifted towards a lower angle and showed splitting. Since the barium atom is a transition-metal element, there is a major state of being in the +2 for Ba ion after the high-temperature sintering process of PMN-0.35PT ceramics. From the ionic radii point of view, the ionic radius of Ba^{2+} (R_{Ba}^{2+} = 1.61 Å) is too large for the ions to enter into A-site ions (R_{Pb}^{2+} = 1.49 Å) [18–20]. Besides, the coordination number of Ba ion is known to be six, which is in great contrast to the coordination number (twelve) of Pb^{2+} ions in the A-site of PMN-0.35PT perovskite.

Table 1 shows the lattice parameters and unit cell volumes of the PMN-0.35PT ceramics with different Ba-doped content. The lattice parameters and unit cell volumes of the Ba-doped 0.65PMN-0.35PT ceramics were calculated with the Rietveld method based on the XRD patterns shown in Fig. 1. It was calculated by assuming that all the Ba ions dope into Rhombohedral (PMN) and Tetragonal (PT), respectively. The results are listed in Table 1. It can be seen from the table that the cell parameters of both PMN and PT increase with the increasing Ba ion content.

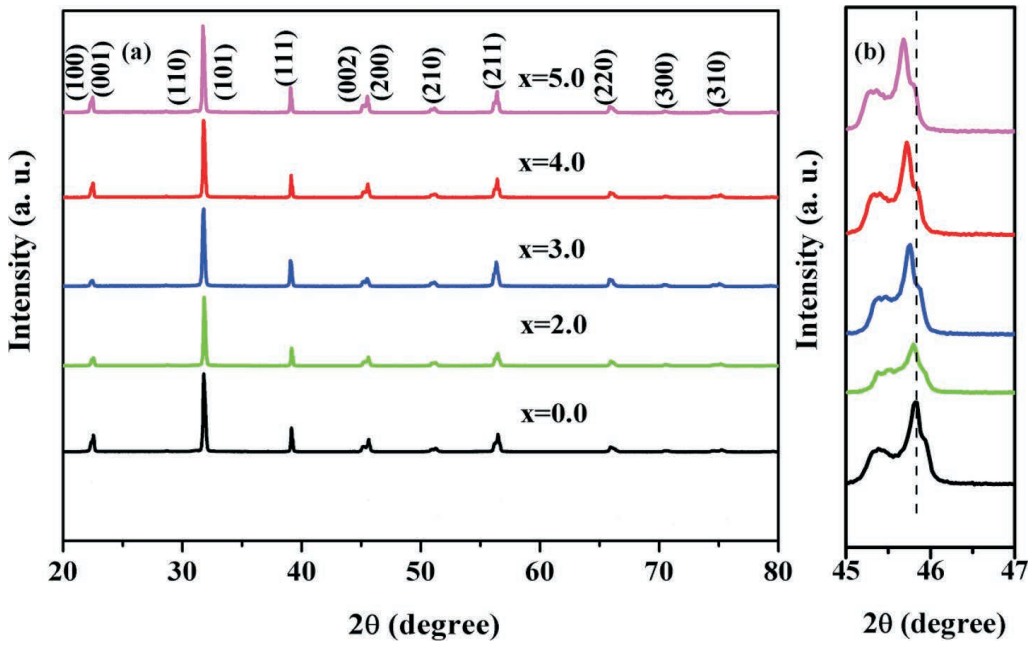

Fig. 1: (a) XRD patterns of Ba-doped PMN-0.35PT ceramics (x = 0.0, 2.0, 3.0, 4.0 and 5.0 mol%) and (b) the locally magnified (200) diffraction peaks at 2θ ≈ 45.8°.

Table 1: The lattice parameters (Å) and unit cell volumes of the Ba-doped 0.65PMN-0.35PT ceramics were calculated with the Rietveld method based on the XRD patterns.

	Phase			
	Rhombohedral	**Volume**	**Tetragonal**	**Volume**
Ba^{2+} (mol)		(Rhombohedral)		(Tetragonal)
0.00	a=b=c=3.984814	63.2738	a=b=3.984198 c=4.009967	63.6536
0.02	a=b=c=4.013767	64.6630	a=b=4.002034 c=4.013526	64.2817
0.03	a=b=c=4.016848	64.8121	a=b=4.009907 c=4.017867	64.6047
0.04	a=b=c=4.022980	65.1094	a=b=4.027719 c=4.036801	65.4871
0.05	a=b=c=4.027443	65.3263	a=b=4.029967 c=4.042463	65.6522

The unit cell volumes of both rhombohedral and tetragonal also increase correspondingly. According to Bragg Law, 2d sin (θ) = λ, the observed diffraction peak shifting to a small angle is the result of the increase of the lattice parameters caused by Ba doping.

Fig. 2(a, b, c, d and e, respectively) shows the typical SEM micrographs of PMN-0.35PT ceramics with different amounts of Ba ion, and Fig. 2f shows the average grain size and relative density of PMN-0.35PT ceramics with different amounts of Ba ion. In contrast to the uneven and small grain size of undoped ceramic, the grain of Ba-doped ceramics is well developed. The average grain size increases from 5.5 μm for undoped ceramic to nearly 10 μm for Ba-doped ceramics. The measured relative density of ceramics firstly decreases slightly with the increasing Ba ion content from 0 mol% to 2 mol%, then clearly increases to a maximum with a Ba content of x = 3.0 mol%, with a density value of 7.80 g/cm^3, which corresponds to about 94.30 % of the theoretical density (ϱ_{theo} = 8.14 g/cm^3 [21]). The relative density of the ceramics decreases almost linearly with the increasing Ba content from 3 mol% to 5 mol%. This is mainly explained by the fact that lead and barium dioxides would form a liquid phase to facilitate densification during the early and middle stages of sintering. However, the Ba dopant has a solubility limit in PMN-0.35PT. The excessive Ba dopant presumably segregates in the grain boundary, which leads to a reduction of density at x = 4.0 mol%. SEM/EDS analysis was conducted on the fractured surface of PMN-0.35PT ceramics doped with Ba at 4.0 mol%. The EDS spectrum was acquired at different spots along the grain boundary, and the corresponding elemental compositions were calculated. The SEM image and EDS spectrum are shown in Fig. 3, and the elemental compositions are listed in Table 2.

As shown in Table 2, the Ba atom content varies significantly across the fractured surface of the grain. It increases from 1.32 % at Spot 1 in the grain center to 4.10 % at Spot 5 close to the boundary. It implies that, with the increase of Ba-dopant, some of the Ba ions might be segregated in the grain boundary, which leads to a reduction in density at x = 4.0 mol% and x = 5 mol%.

(2) Ferroelectric phase transition and large strain response at low electric field

The polarization hysteresis (P-E) loops of PMN-0.35PT ceramics with different Ba-doped content are shown in Fig. 4. As shown in Fig. 3a, when x = 0 mol%, there are saturated hysteresis loops, which are typical for normal ferroelectrics. With the increase of the Ba content to x = 2 mol%, the remnant polarization decreased rapidly at room temperature. The amplitude falls fast from 27.5 μC/cm^2 at 0 mol% to 12.5 μC/cm^2 at 2 mol% (as shown in Fig. 3b). According to reference [16], a sharp decrease in the remnant polarization in PMN-PZN-PNN-PT ceramics was also noticed at about 2.5 mol% Ba-doping. The authors attribute it to the incomplete substitution of Pb^{2+} ions by the Ba^{2+} ions, and the fact that the domain walls are pinned on the crystal structure defects. We think that the two systems have similarities. Then the change becomes much more slight beyond 2 mol% Ba doping. When x = 5 mol%, the remnant polarization reaches its maximum. This is connected with small lattice distortions in the phase, which can be observed by means of X-ray analysis (Fig. 1). These small lattice distortions lead to easier domain switching.

The bipolar strain (S-E) loops at a frequency of 0.1 Hz for Ba-doped PMN-0.35PT ceramics are shown in Fig. 5, which demonstrate the typical butterfly-like strain. During the electric-field-induced phase transition in PMN-0.35PT-based ceramics, a large electrostrictive response could always be found owing to the growth and mobility of the domains or the domain walls [18, 19, 22].

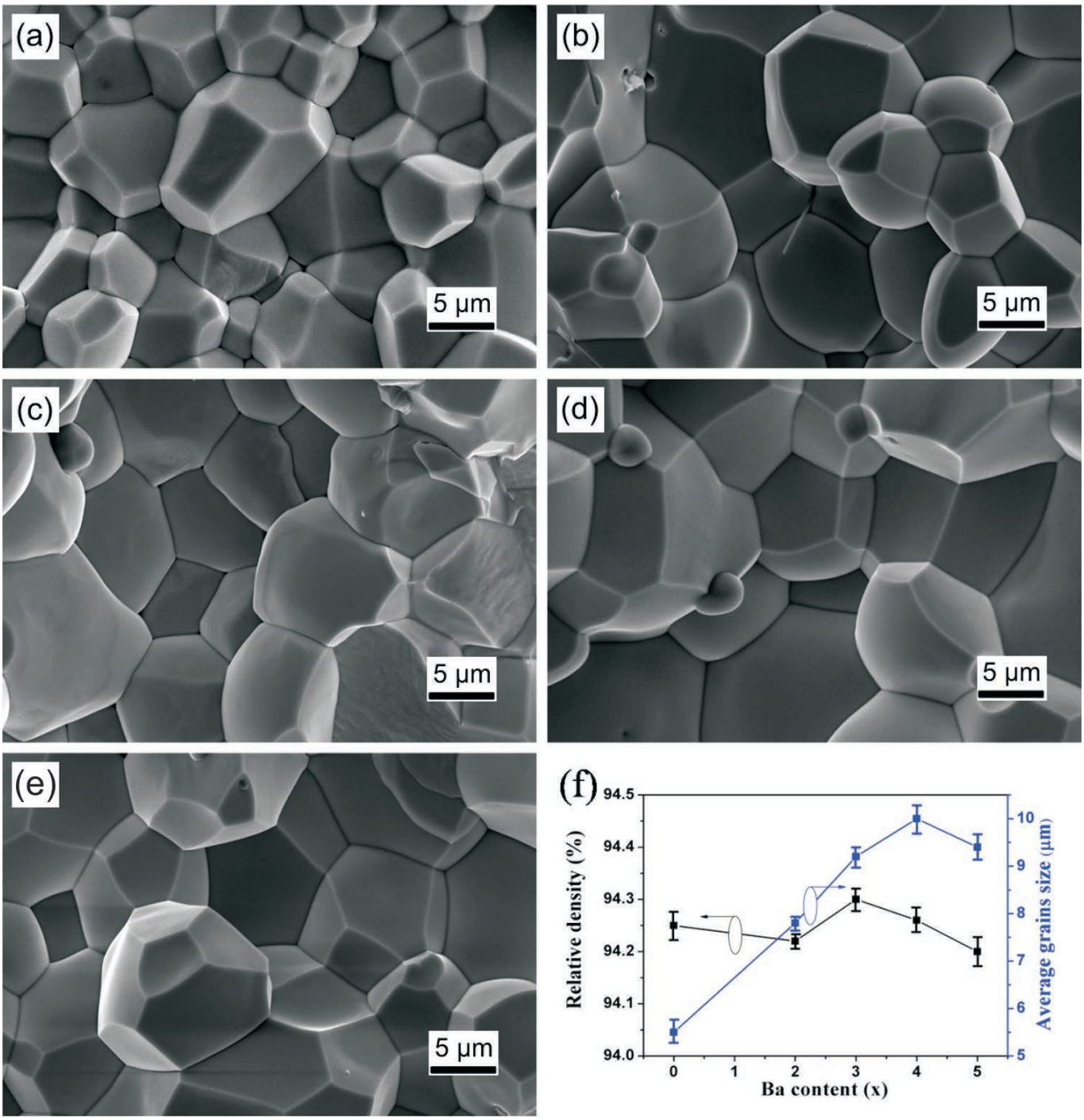

Fig. 2: SEM micrographs of the fractured surfaces of Ba-doped PMN-0.35PT ceramics with (a) x = 0.0, (b) x = 2.0, (c) x = 3.0, (d) x =4.0 and (e) x = 5.0 mol%; and (f) the relative density and the average grains size are plotted as a function of Ba content (x).

Table 2: Atomic ratio calculated from EDS of spots marked in Fig. 3(a).

Atom (%)	Spot				
	1	**2**	**3**	**4**	**5**
Mg K	7.69	5.90	2.26	5.67	6.54
Ti K	18.60	19.96	17.48	15.60	16.01
Nb L	27.96	29.09	33.34	30.19	30.46
Ba L	1.32	2.25	2.31	2.78	4.10
Pb L	44.43	42.79	44.27	45.76	42.89
Total	100	100	100	100	100

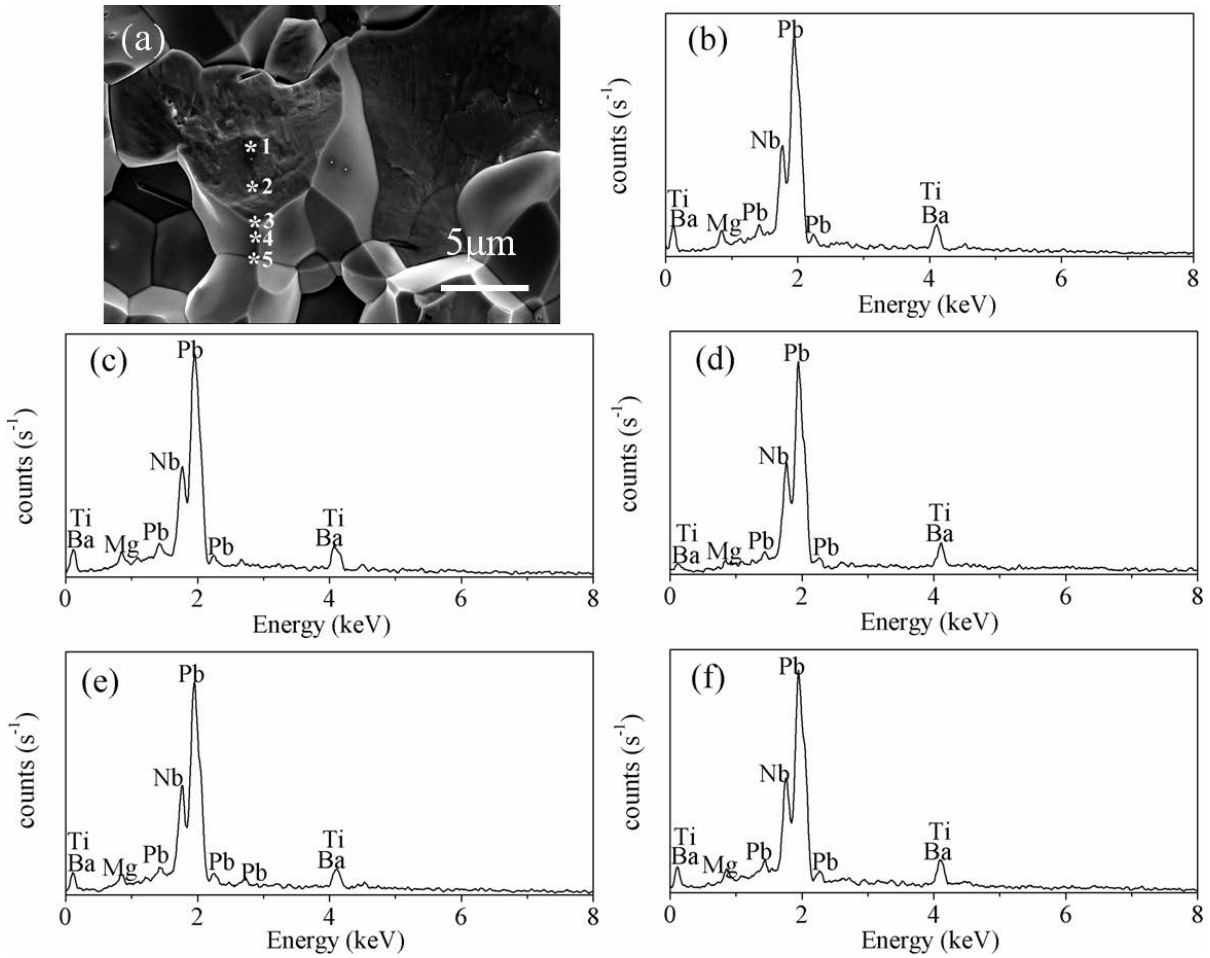

Fig. 3: (a) SEM/EDS of PMN-0.35PT ceramics doped with Ba at 4.0 mol%. (a) SEM image of fractured surface and spots for acquiring EDS spectrums. (b)~(f) EDS spectrums corresponding to Spot 1 to Spot 5 in Fig. 3(a).

The maximum strain response of 0.08 % was obtained for pure PMN-0.35PT ceramic. With a constant addition of Ba dopant, S_m shows a linear increase and obtains an optimum value of 0.13 % at x = 3 mol%. When x = 0 mol%, a bipolar curve with a significant lag is observed, which is typical for normal ferroelectrics. With the increase of the Ba ion content, there is an electric-field-induced phase transition, which was found in the previous study of x = 0.05 mol% ceramics [16]. Ultimately, the strain response of doped ceramics undergoes a great enhancement because of the increasing domain switching.

(3) Piezoelectric properties

Fig. 6 shows the piezoelectric charge coefficients d_{33} of PMN-0.35PT-xBa ceramics as a function of the Ba content. With increasing of Ba ion content, the piezoelectric constant d_{33} shows an increasing trend. The maximum piezoelectric performance is found at x = 0.05 mol% (d_{33} = 508pC/N). The existence of maxima in the concentration dependences of the piezoelectric parameters may be due to two processes. On one hand, the coexistence of the two phases results in a significant number of possible domain configurations; this simplifies the domain reorientation

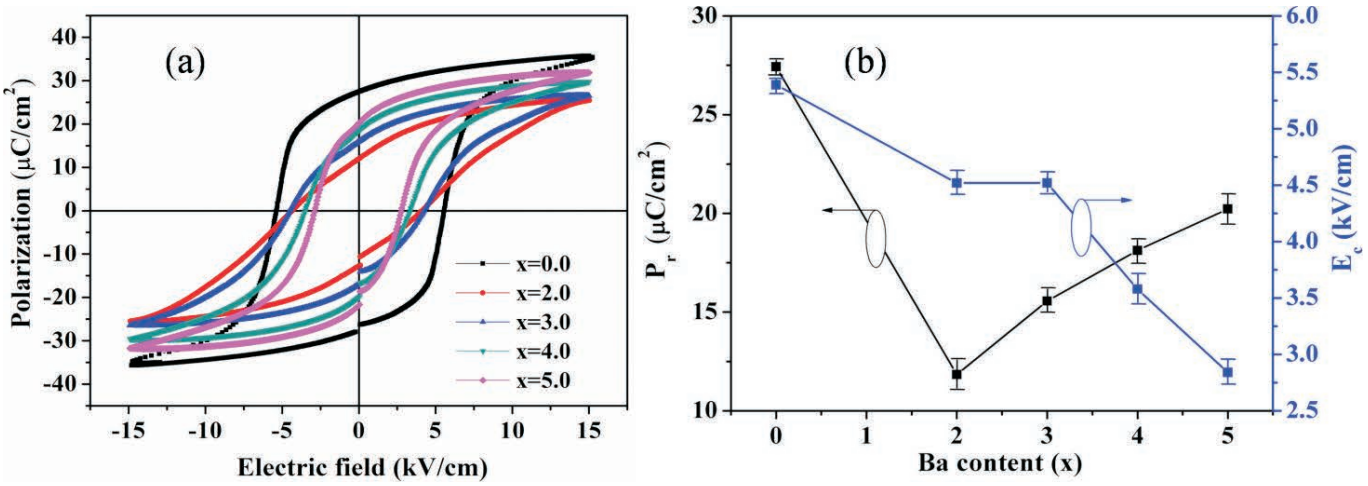

Fig. 4: (a) The polarization-electric field (P-E) hysteresis loop for Ba-doped PMN-0.35PT ceramics, and (b) the variations of remnant polarization (P_r) and coercive field (E_c) as a function of Ba content(x).

processes and results in an increase in the electromechanical response. On the other hand, with the increasing Ba ion content, the phase transition leads to the increase of its piezoelectric properties [16].

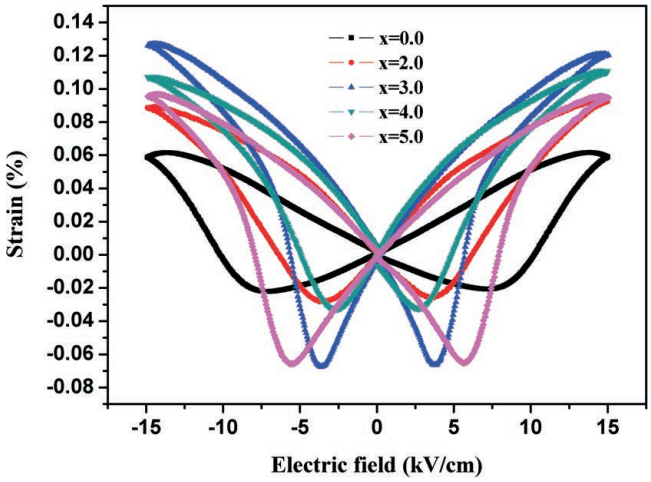

Fig. 5: The bipolar strain (S-E) curves for Ba-doped PMN-0.35PT ceramics.

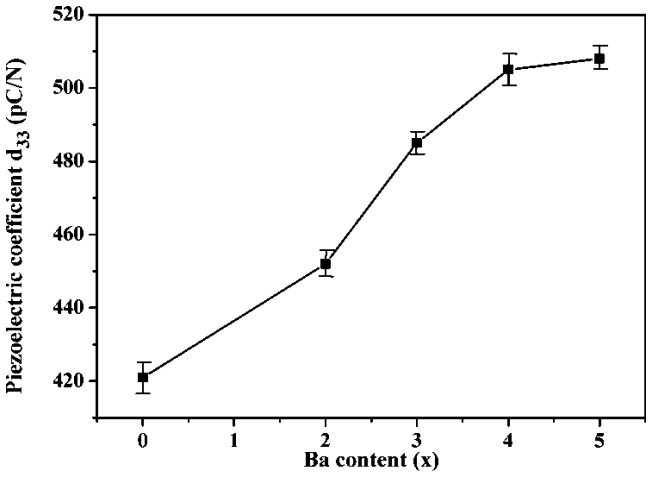

Fig. 6: Piezoelectric charge coefficients d_{33} of Ba-doped PMN-0.35PT ceramics.

IV. Conclusions

Ba-doped PMN-0.35PT relaxor-based ferroelectric ceramics were prepared with a two-step columbite precursor method. When Ba dopant was added, the density of the PMN-0.35PT ceramics increased accompanied by a homogeneous and larger grain size. Ba-doped ceramic with optimal density of 7.78 g/cm^3 was obtained at x = 3.0 mol%, and its average grain size is approximately 9.3 μm. Owing to the substitution of Ba ions for A-sites in the PMN-0.35PT perovskite structure, the phase structure of Ba-doped ceramics was profoundly modified, resulting in the changes in the electrical properties. With addition of an appropriate amount of Ba dopant to the PMN-0.35PT ceramic, the piezoelectric, ferroelectric and electrostrictive responses were significantly improved. The PMN-0.35PT ceramic doped with 3.0 mol% Ba content gave the optimum S_m of 0.13 % at 15 kV/cm at room temperature. When x = 5.0 mol%, its piezoelectric constant d_{33} reaches 508pC/N (Fig. 6).

Acknowledgments

This work was supported by the Major Program for the Natural Scientific Research of Jiangsu Higher Education Institutions (12KJA430002) and Priority Academic Program Development (PAPD) of Jiangsu Higher Education Institutions. The authors acknowledge the financial support from the Program for Chang jiang Scholars and Innovative Research Team in University (PCSIRT), IRT1146.

References

1 Cross, L.E.: Relaxor ferroelectrics, *Ferroelectrics*, **76**, 241 – 267, (1987).

2 Swartz, S.L., Shrout, T.R., Schulze, W.A., Cross, L.E.: Dielectric-properties of lead-magnesium niobate ceramics, *J. Am. Ceram. Soc.*, **67**, 311 – 315, (1984).

3 Shvartsman, V.V., Kholkin, A.L.: Domain structure of 0.8Pb-$Mg_{1/3}Nb_{2/3}O_3$-0.2$PbTiO_3$ studied by piezoresponse force microscopy, *Phys. Rev. B*, **69**, 014102, (2004)

4 Shrout, T.R., Schulze, W.A., Biggers, J.V.: Dielectric behavior of single crystals near the (1-x) $Pb(Mg_{1/3}Nb_{2/3})O_3$-(x) $PbTiO_3$ morphotropic phase boundary, *Ferroelectrics Lett.*, **12**, 63 – 69, (1990).

5 Xi, Z., Hou, Z., Li, X., Fang, P., Long, W.: Study on structure and properties of $Pb(Sc_{1/2}Nb_{1/2})O_3$-$Pb(Mg_{1/3}Nb_{2/3})O_3$-$PbTiO_3$ ternary ceramics near morphotropic phase boundary, *Ceram. Int.*, **41**, S787 – S791, (2015).

6 Chae, M.-S., Koh, J.-H.: Piezoelectric behavior of (1-x)($PbMgNbO_3$-$PbZr\,TiO_3$)-x($BaTiO_3$)ceramics for energy harvester applications, *Ceram. Int.*, **40**, 2551 – 2555, (2014).

7 PhamThi, M., Augier, C., Dammak, H., Gaucher, P.: Fine grains ceramics of PIN-PT,PIN-PMN-PT and PMN-PT systems:drift of the dielectric constant under high electric field, *Ultrasonics*, **44**, e627 – e631, (2006).

8 Hosono, Y., Yamashita, Y., Sakamoto, H., Ichinose, N.: Dielectric and piezoelectric properties of $Pb(In_{1/2}Nb_{1/2})O_3$-$Pb(Mg_{1/3}Nb_{2/3})O_3$-$PbTiO_3$ ternary ceramic mterials near the morphotropic phase boundary, *Jpn. J. Appl. Phys.*, **42**, 535 – 538, (2003).

9 Noheda, B., Cox, D.E., Shirane, G., Gao, J., Ye, Z.G.: Phase diagram of the ferroelectric relaxor(1-x)$Pb(Mg_{1/3}Nb_{2/3})O_3$-x$PbTiO_3$, *Phys. Rev. B*, **66**, 054104, (2002).

10 Jiang, T., Li, Q., Yan, Q., Luo, N., Zhang, Y., Chu, X.: Composition and temperature dependence of ferroelectric and pyroelectric properties of (1-x)[PMN-PT(65/35)]-xPZ ($0 \le x \le 0.10$)ceramics, *Mater. Res. Bull.*, **59**, 421 – 424, (2014).

11 Qi, X., Sun, E., Wang, J., Zhang, R., Yang, B., Cao, W.: Electromechanical properties of Mn-doped $Pb(In_{1/2}Nb_{1/2})O_3$-$Pb(Mg_{1/3}Nb_{2/3})O_3$-$PbTiO_3$ piezoelectric ceramics, *Ceram. Int.*, **42**, 15332 – 15337, (2016).

12 Nomura, S., Kaneta, K., Kuwata, J., Uchino, K.: Recent applications of PMN-based electrostrictors, *Ferroelectrics*, **50**, 197 – 202, (1983).

13 Zhong, N., Xiang, P.-h., Sun, D.-z., Dong, X.-l.: Effect of rare earth additives on the microstructure and dielectric properties of $0.67Pb(Mg_{1/3}Nb_{2/3})O_3$-$0.33PbTiO_3$ ceramics, *Mater. Sci. Eng. B*, **116**, 140 – 145, (2005).

14 Zhao, X., Qu, W., He, H., Vittayakorn, N., Tan, X.: Influence of cation order on the electric field-induced phase transition in $Pb(Mg_{1/3}Nb_{2/3})O_3$-based relaxor ferroelectrics, *J. Am. Ceram. Soc.*, **89**, 202 – 209, (2006).

15 Ling, H.C., Yan, M.F., Rhodes, W.W.: Lead zinc niobate Pyrochlore: structure and dielectric properties, *J. Mater. Sci.*, **24**, 541 – 548, (1989).

16 Talanov, M.V., Shilkina, L.A., Verbenko, I.A., Reznichenko, L.A.: Impact of Ba^{2+} on structure and piezoelectric properties of PMN-PZN-PNN-PT ceramics near the morphotropic phase boundary, *J. Am. Ceram. Soc.*, **98**, 838 – 847, (2015).

17 Augustine, P., Samanta, S., Rath, M., *et al.*: Stabilization heat treatment and functional response of $0.65[Pb(Mg_{1/3}Nb_{2/3})O_3]$ -$0.35[PbTiO_3]$ ceramics, *Mater. Res. Bull.*, **95**, 47 – 55, (2017).

18 Shannon, R.D., Prewitt, C.T.: Effective ionic radii in oxides and fluorides, *Acta Crystallogr. B*, **25**, 925 – 946, (1969).

19 Lee, K.-M., Jang, H.M.: A new mechanism of nonstoichiometric 1:1 short-range ordering in NiO-doped $Pb(Mg_{1/3}Nb_{2/3})O_3$ relaxor ferroelectrics, *J. Am. Ceram. Soc., 81, 2586 – 2596, (1998).*

20 Chen, G., Zhang, Y., Chu, X.-M., *et al.*: Large electrocaloric effect in La-doped $0.88Pb(Mg_{1/3}Nb_{2/3})O_3$-$0.12PbTiO_3$ relaxor ferroelectric ceramics, *J. Alloy Compd.*, **727**, 785 – 791, (2017).

21 Bruno, J.C., Cavalheiro, A.A., Zaghete, M.A., Cilense, M., Varela, J.A.: Structural effects of Li and K additives on the columbite precursor and 0.9PMN-0.1PT powders, *Mater. Chem. Phys.*, **84**, 120 – 125, (2004).

22 Bokov, A.A., Ye, Z.G.: Recent progress in relaxor ferroelectrics with perovskite structure, *J. Mater. Sci.*, **41**, 31 – 52, (2006).